scientific reports

Check for updates

OPEN

Urban heat island linkages with the landscape morphology

T. V. Ramachandra[1,2,3,6]✉, Rajesh Singh Rana[1,4,6], S. Vinay[1,5,6] & Bharath H. Aithal[1,4,6]

The landscape consists of a mosaic of interacting ecosystem elements, which maintain stability and aid in sustaining crucial services. Unplanned developmental activities leading to the transition of pervious surfaces into impervious/paved surfaces have significant implications for the urban climate, mainly through the phenomenon of urban heat islands (UHIs). Changes in landscape integrity could be quantified through land use (land cover) assessment and urban heat island effect through spatial computation of land surface temperature (LST). The current research uses multi-resolution remote sensing data to evaluate UHIs with landscape dynamics and assess the complex spatial interrelationships in heterogeneous urban landscapes at micro-levels. The composition of pervious and impervious surfaces at the micro-level plays a pivotal role in regulating thermal comfort. Landscape configuration at microlevels, predominantly barren (C1 class) and urban (C2 class) areas, constitute hotspots with higher temperatures. UHI was mapped through the urban hotspot and Urban thermal field variance index (UTFVI) analysis. Urban hotspot analysis shows the 15.41 km^2 area in the city has a very high temperature. The study provides vital data-driven insights into the complex relationship between urban land use and LST at the micro-level that supports the decision-makers, stakeholders, and public officials in policymaking.

Keywords Landscape dynamics, Land surface temperature (LST), Urban heat island (UHI), Spatial interrelationship, Urban thermal field variance index (UTFVI)

Urbanization and urban growth

Urban areas are the cradles of human societies, and evolution can be traced back to the river valley civilizations[1]. The economic status of metropolitan areas was predominantly agrarian, which transitioned to an industry-based economy during the eighteenth century with the Industrial Revolution. Urbanization is a dynamic, complex phenomenon involving large-scale changes in land uses at local levels. Human-induced land use (LU) changes have been the major driver of changes in regional and global environments[2]. Urbanization patterns directly influence the urban growth process, which extends their influence on the neighborhood, resulting in sprawl or peri-urban growth. Urban growth is a spatial and demographic process that leads to the concentration of the human population with a higher level of economy. The impetus of industrialization to urbanization led to the transformation of rural landscapes into paved surfaces with buildings (residential and commercial), roads, and factories[2]. Urbanization resulted in the growth of towns and cities, which formed an economic hub by setting up industries and institutions with better living standards, employment prospects, education access, health care, etc[2,3]. Population projections indicate that 55.3% of the global population in urban areas (in 2018) is expected to increase to 68.4% by 2050[4].

Compact cities have been promoted in urban planning and development since the early 1990s for contributing to the economic, environmental, and social goals of sustainability[5,6]. However, subsequently, the economic goals dominated, leading to rapid urbanization with unplanned developmental activities, which compromised the environmental and social goals[7,8], evident from increased traffic congestion, enhanced temperature, higher greenhouse gas footprint, reduced worker productivity, less affordable housing, loss of property rights, reduced geographic mobility, higher housing costs, lower homeownership rates, reduced economic mobility, higher consumer costs, and reduced urban services.

[1]Energy & Wetlands Research Group and IISc-EIACP, Centre for Ecological Sciences [CES], Indian Institute of Science, http://wgbis.ces.iisc.ac.in/energy. [2]Centre for Sustainable Technologies [astra], Indian Institute of Science, Bangalore 560012, India. [3]Centre for Infrastructure, Sustainable Transportation and Urban Planning [CiSTUP], Indian Institute of Science, Bengaluru 560012, Karnataka, India. [4]Ranbir and Chitra Gupta School of Infrastructure Design and Management, Indian Institute of Technology, Kharagpur, India. [5]Geoinformatics Research Lab, Department of Civil Engineering, Alva's Institute of Engineering and Technology, Moodbidri, India. [6]T. V. Ramachandra, Rajesh Singh Rana, S. Vinay and Bharath H. Aithal contributed equally to this work. ✉email: energy.ces@iisc.ac.in; tvr@iisc.ac.in; envis.ces@iisc.ac.in

Rapid urbanization, allowing population influx beyond the carrying capacity of a region, strained natural resources, which contributed to a lack of basic amenities, housing shortages, water scarcity, insufficient infrastructure, and escalated pollution, which has been impacting the overall quality of life. The transition of the porous landscape (with vegetation, water bodies, and open spaces) to paved surfaces (with buildings, roads, etc.) has contributed to (i) the decline of vegetation, surface water bodies, and groundwater recharge capability, (ii) frequent heat waves with the enhanced land surface temperature (LST), due to unique heating and radiation capabilities of artificial surfaces (paved surfaces such as roads, etc.). LST constitutes the surface temperature of a landscape, which is the manifestation of atmospheric interaction and energy fluxes between the atmosphere and the Earth. LST controls sensible and latent heat flux exchange, which plays a pivotal role in the landscape processes[9–12].

Background of urban heat island (UHI)

The alteration in the landscape structure driven by anthropogenic land use changes with the increase in paved surfaces (urbanized areas) at the expense of porous surfaces (vegetation cover, water bodies, etc.) have resulted in socio-environmental impacts[13]. Rapid urbanization has enhanced the spatial extent of impervious surfaces (Buildings, roads, glass facades, industries, etc.) with high absorption and emission rates for solar radiation and low albedo. A high amount of emitted solar energy from urban landscapes affects the temperature and surface energy balance, which can have several adverse effects like urban heat island (UHI) and consequent prevalence of vector-borne diseases with air, water, and land pollution[14]. Urban areas emit higher temperatures than surrounding non-urban areas (natural areas) due to high energy emission with heat accumulation from anthropogenic activities and heat transfer from other sources, and this phenomenon is referred to as the urban heat island (UHI) effect[15–17]. UHI is the effect where, due to high energy emission, the temperature of impervious surfaces in urban areas is elevated compared to that of neighboring non-urban natural areas. Urban areas in tropical and subtropical climate regions are more vulnerable to UHI than those in temperate (colder) climates[18]. Heatwave exposure in urban areas has increased disproportionately in developing countries consequent to globalization compared to developed economies[19], highlighting the linkages of economic disparities with UHI dynamics[20–22]. Environmental degradation poses severe challenges in developing countries with limited adaptive capacity, and these regions are vulnerable to adverse impacts of increasing temperature[15,23]. Hence, the current research underscores the urgent need to address climate vulnerabilities at disaggregated levels in developing countries to ensure consideration of urban thermal complexities for developing location-specific climate-resilient urban systems.

UHI reduces thermal comfort, increasing energy utilization and pollution levels[24]. The increasing urban densities coupled with changes in the climate have aggravated heat waves with stress-based morbidity and mortalities in major cities[25]. The spatial configuration of the urban forms and their influence on the heat dynamics depict the linkage between urban heat islands and landscape morphology. Compact cities with high-density urban development intensify urban heat island (UHI) effects due to the accumulation of impervious surfaces, reduced vegetation, and limited airflow caused by closely situated urban edifices[5,6]. These variables enhance heat retention and diminish natural cooling processes, intensifying localized temperature elevations[5,6,24]. Nevertheless, the extensive spatial urban footprint linked to decentralized forms enlarges the expanse of impervious surfaces, thereby exacerbating regional-scale urban heat island effects while elevating energy consumption and transportation emissions[25]. In contrast, urban growth, marked by reduced density with the scattered spatial arrangements, alleviates localized UHI due to improved airflow and the presence of heat sinks (vegetation cover and waterbodies)[2,13,26].

UHI has been quantified with outdoor ambient air and land surface temperature obtained from meteorological stations and thermal spatial data (remote sensing data)[27]. However, the lack of meteorological stations at disaggregated levels makes it difficult to estimate the UHI with air temperature. In this context, thermal spatial data acquired through space-borne sensors at regular intervals provides an effective way to monitor land surface temperature (LST) as it indicates the surface energy balance, which directly affects the urban environment. Moderate-resolution sensors (ASTER, MODIS, etc.) and high-resolution (Sentinel-2, Landsat, etc.) are commonly used to assess the effect of land use changes on the thermal environment.

Urban dynamics and UHI through geoinformatics: existing methods and limitation

Moderate-resolution (ASTER, MODIS, etc.) and high-resolution (Sentinel-2, Landsat, etc.) sensors are commonly used to assess the effect of land use changes at regional levels. These spatial data of different satellites come with a trade-off between spatial and temporal resolution, such as MODIS, Landsat (5–8), AVHRR, and ASTER, with spatial resolution ranging between 30 m and 1 Km and temporal resolution ranging from day to month. The low spatial and high temporal resolution (MODIS, AVHRR) thermal bands are apt for studying the large area, and high spatial and low temporal resolution (ASTER and LANDSAT) are appropriate for estimating the UHI at a regional scale.

Spatial data of different satellites comes with a trade-off between spatial and temporal resolution, such as MODIS, Landsat (5–8), AVHRR, and ASTER, with spatial resolution ranging between 30 m and 1 Km and temporal resolution ranging from day to month. The low spatial and high temporal resolution (MODIS, AVHRR) thermal bands are apt for studying the large area, and high spatial and low temporal resolution (ASTER and LANDSAT) are appropriate for estimating the UHI at a regional scale.

Exploring the spatial pattern of Urban Heat Island (UHI) is crucial for understanding how the distribution of Land Use/Land Cover (LULC) and its changes impact Land Surface Temperature (LST). Therefore, it is essential to investigate the relationship between LULC changes and corresponding variations in LST. Several studies have shown the change in LST concerning LULC such that LULC change with LST from 1991 to 2021 in Durgapur (India) reveals an increase in the minimum and maximum LST values from 18.39 °C to 22.92 °C and from

31.65 °C to 44.60 °C T with the rise in urban, mining, and agriculture areas and decline of vegetation have increased[28]. Comparative assessment of LST in a planned (Kalyani City) and an unplanned city (Barasat City) in West Bengal using LANDSAT data from 2005 to 2019 shows that the built-up area in the planned city increased from 47.41 to 54.97%, while the unplanned city witnessed an increase in built-up from 42.16 to 65.56%[1] highlighting an increase of 8% compared to the rise of 2.65% in planned cities. Assessment of the effect of urban factors on LST and outdoor air temperature (OAT) in Seoul illustrates that land use characteristics influenced LST, while urban morphological characteristics influenced OAT[27]. Evaluation of 2D and 3D structures on LST in Tartu, Estonia, reveals the urban hot spots in areas with higher mean height of impervious surfaces compared to the cold spots in higher mean vegetation regions[29]. The regression analysis of urban spatial factors and LST using the Random Forest algorithm highlights a positive and linear correlation of building density with LST, compared to a negative and non-linear pattern with the mean compactness factor and mean building height[30]. A multivariate analysis of LST and four different spectral indices in Bogura (Bangladesh) demonstrates the increase of LST across urban and rural functions[31].

Grid-wise temporal analyses of the correlation between spectral indices and LST[32] revealed a negative correlation between LST-NDVI and NDVI-NDBI. In contrast, a positive correlation was found between LST-NDBI and LST-UTFVI. A study on the role of urban trees in mitigating the rise of LST among 293 European cities[33] shows that urban trees exhibit lower temperatures than urban fabric across most European cities. The LST difference between urban trees and continuous urban fabric is high in Central Europe (8 to 12 °K). In comparison, it is low in Southern Europe (0 to 4 °K). Assessment of the landscape dynamics in the Bengaluru Urban district and Bengaluru City from 1973 to 2022 using temporal remote sensing data highlights that the built-up cover of Bengaluru Urban district has increased from 3.85 to 55.71% while the built-up cover of Bengaluru city has increased from 8.05 to 86.63%, highlighting of rapid urbanization with profound environmental implications in the neighboring areas[34]. Investigations of morphological characteristics of built-up areas and surface heat islands in Shenzhen city reveal that the UHI intensity is positively correlated to the proportions of core, edge, and bridge of the built-up regions but negatively connected to the proportion of vegetation cover[35–37]. The spatial pattern of the built-up areas influences surface urban heat islands[37].

Significance of micro-level analyses of LST with LU

Multiple studies (discussed earlier[5,6,13] to[37]) highlight the relationship between landscape structure (manifested by land use) and land surface temperature (LST). These studies often emphasize comprehensive patterns and broader ideas, but investigations are scanty of the complex spatial interrelationships at the micro level in heterogeneous urban landscapes. Landscapes marked by different land uses, differing building densities, and fragmented green spaces necessitate a more sophisticated comprehension to precisely explain the localized dynamics of land surface temperature changes and their relationship to particular land use attributes. The review of published literature highlights the need to investigate variations in land uses at a sub-pixel level and their influence on LST, and these influences can be effectively quantified using high-resolution optical remote sensing data with thermal data. In this context, the current study investigated the complex relationship between the LST and land use dynamics using LANDSAT-8 (30 m spatial resolution, thermal data)[38] and Sentinel-2 (10 m spatial resolution, optical data)[39] in Bengaluru city which has been undergoing severe environmental and ecological transitions due to the rapid urbanization leading to a loss of vegetation, open spaces, and water bodies. A pixel of 30 m spatial resolution (Landsat) would cover 9 pixels of 10 m spatial resolution (Sentinel), which aided in assessing LST (thermal pixel) with land uses at disaggregated levels.

Study objectives and novelty

The objectives of the study are (i) to understand the landscape dynamics through land use changes during five decades using temporal (from 1973 to 2025) remote sensing data, (ii) to assess the relationship between LST and different spectral indices of land cover, and (iii) analyze the linkages of LST with land uses at micro-levels. The current investigation of UHI with LU at the micro-level (proportion-based analysis) is a novel approach and contributes significantly to the UHI research domain and policy advocacy.

Results

Land use dynamics

Land uses assessed using temporal remote sensing data (from 1973 to 2025) through supervised non-parametric classifier based on the Random Forest algorithm reveal rapid urbanization with a 1078% increase in urban (built-up) area (Fig. 1) as evidenced by the dramatic increase in built-up area from 7.97% (1973) to 87.64% (2025) during the last five decades (Supplementary Table S1). Bangalore witnessed spatial expansion in the mid-2000s with the formation of the Greater Bangalore (BBMP) by including adjacent rural landscapes, which led to the conversion of agricultural land to paved areas. The city landscape witnessed a 1078% increase in built-up with a decline of 88% vegetation cover and 79% water bodies, leading to the transition of the landscape from porous to paved surfaces, affecting the hydrology, ecology, and socio-economic aspects.

The urban trajectory in Bangalore city exhibits distinct phases (Supplementary Figure S1): (i) From 1973 to 1992, steady annual growth of 1% driven primarily by the establishment of nationalized public sector industries, (ii) globalization and subsequent relaxation in markets during the nineties witnessed the emergence of IT (information technology) sector, (iii) post-2002 era witnessed surge, with annual growth rates surging to 2.01% due to the proliferation of private industries and Special Economic Zones (SEZs). These developments generated employment opportunities and pushed a rapid conversion of peri-urban landscapes for residential and commercial development. (iv) 2012–2021: intense urban growth driven by the increasing IT sector and the associated influx of population and annual urbanization reached 3%. (v) post-2021 witnessed annual

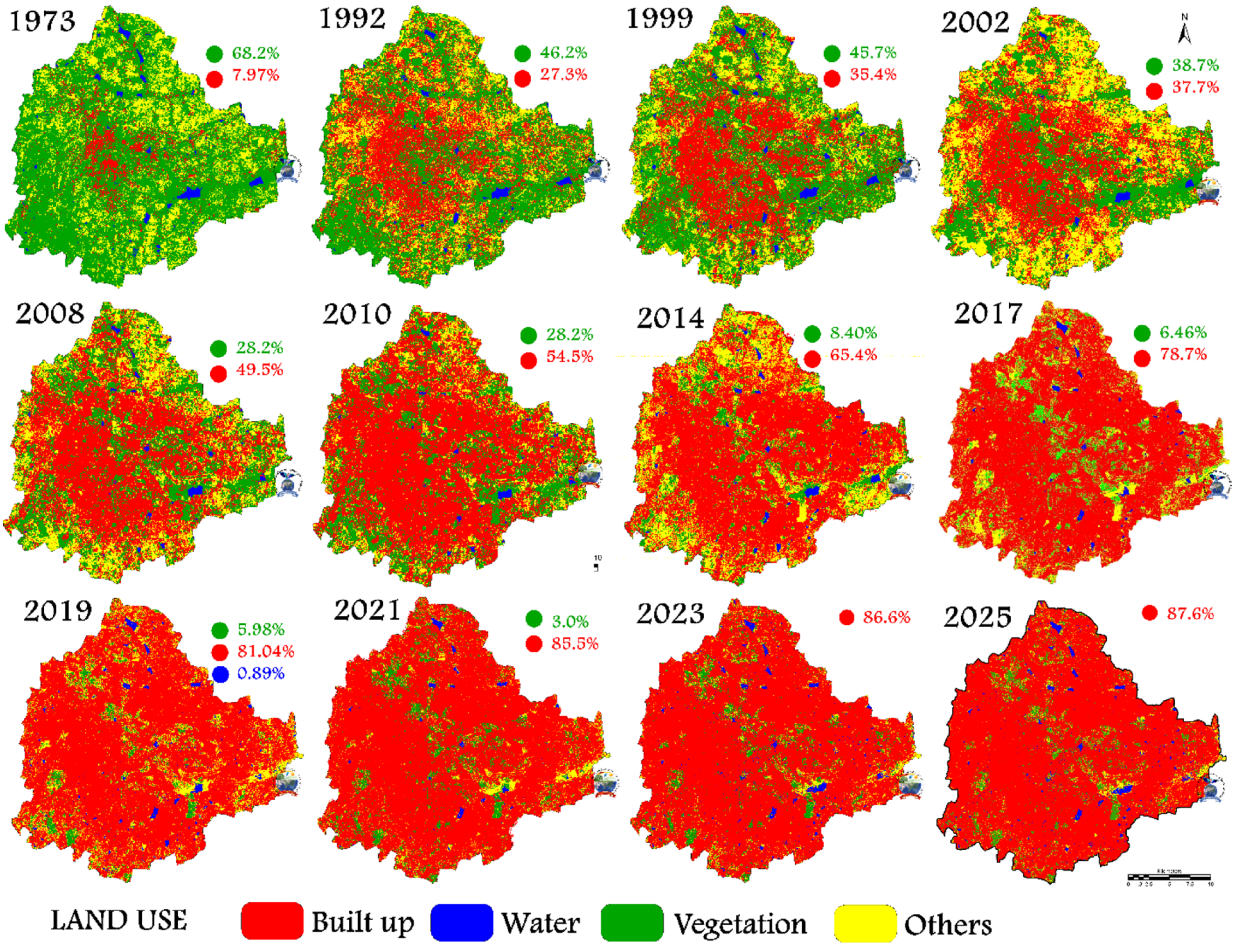

Fig. 1. Landscape dynamics in Bangalore. Created using the open-source software QGIS 3.22 [https://www.qgis.org/] and GRASS GIS 7.8.2 [https://wgbis.ces.iisc.ac.in/grass/].

urbanization of 0.5% with the proliferation of residential layouts and a shift towards lower-density urban sprawl beyond the BBMP engulfing the adjacent agrarian spaces.

Figure 2 depicts the increase in paved surfaces with an exponential decline in natural surfaces (water bodies, vegetation cover, open spaces, etc.). The primary driver of urban expansion during the past five decades is unplanned urbanization, which has led to converting green (agricultural land, etc.) and blue (water bodies) spaces into residential and commercial areas. The urban growth with reference to the time is given by Eq. (1), and the decline of natural surfaces is given by Eq. (2). (Supplementary Table S2). Supplementary Figure S2 illustrates the increase in paved surfaces from 7.97% (in 1973) to 87.64 (in 2025). Urban growth trend analyses reveal that the city landscape is almost near saturation, surpassing carrying capacity. The current path of urbanization has resulted in greenhouse gas (GHG) rich, water-scarce, non-resilient, and unlivable while depriving city dwellers of clean air, water, and the environment.

Probable relationship of urban growth (paved surfaces) and decline of non-built up

$$y = 0.3096\ln(x) + 0.0291 \quad (1)$$

(dependent variable: urban growth (in percentage) and independent variable: year), correlation coefficient: 0.985, $p < 0.05$.

Rate of decline of non-built-up (porous surfaces such as vegetation, water bodies, open spaces, etc.)

$$y = 1.0101e^{-0.14x} \quad (2)$$

(dependent variable: non-built-up decline (in percentage) and independent variable: year), correlation coefficient: 0.993, $p < 0.05$.

LU dynamics assessment highlights that Bangalore has been experiencing unprecedented urbanization and sprawl in recent times due to concentrated developmental activities with the policy impetus on industrialization for the economic development of the region. The focused growth has increased population and consequent pressure on infrastructure natural resources, and ultimately giving rise to a plethora of serious challenges such as climate change, enhanced greenhouse gas emissions, lack of appropriate infrastructure, traffic congestion,

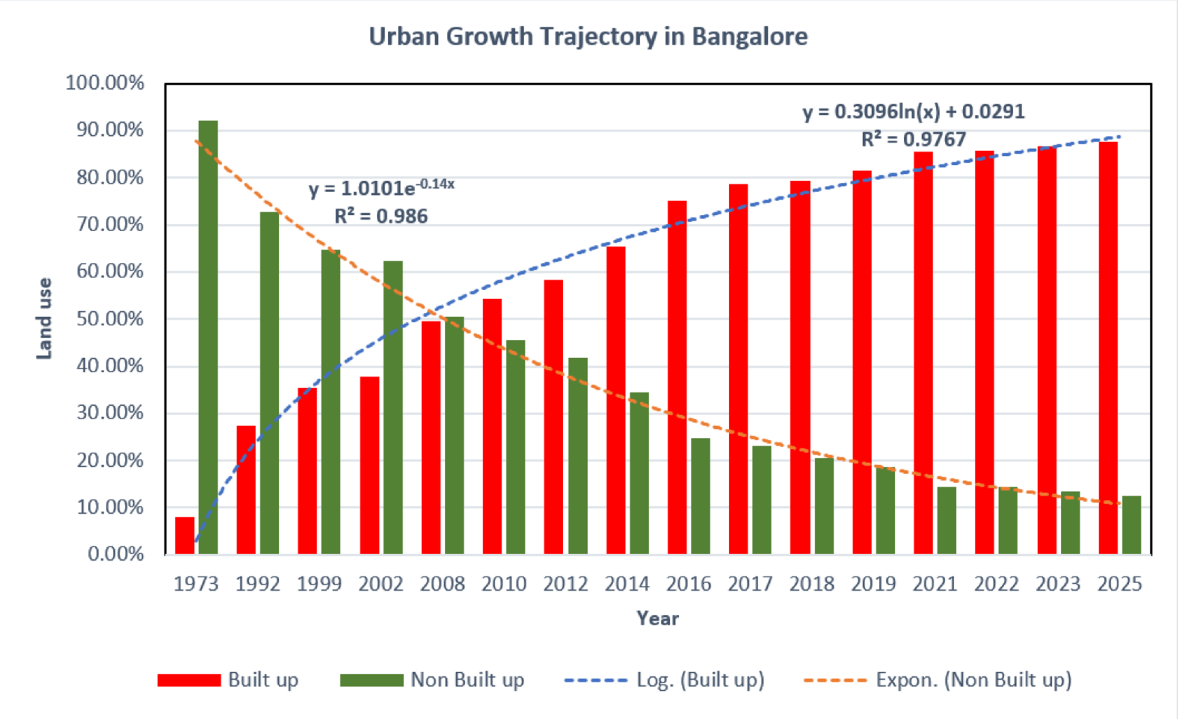

Fig. 2. Urban Growth Trajectory in Bangalore Created using EXCEL with urban dynamics data. Created using the open-source software QGIS 3.22 [https://www.qgis.org/] and Open Office 365.

and lack of basic amenities (electricity, water, and sanitation) in many localities, etc., which necessitated LU assessment at micro levels and linkages with the surface temperature.

Land cover analysis

Land cover is assessed through indices such as Normalized Difference Vegetation Index (NDVI), Normalized Difference Built-up Index (NDBI), Modified Normalized Difference Water Index (MNDWI), and Bare soil Index (BSI) using Sentinel data (10 m resolution) considering spectral bands, which provided the spatial extent of vegetation, built-up, water, and bare soil. Supplementary Figure S3 depicts the spatial extent of vegetation, build-up, water, and bare soil, respectively computed through NDVI, NDBI, MNDWI, and BSI. NDVI shows the area under vegetation is 16.07%, and the area under non-vegetation is 83.93%. NDBI shows the areas under built-up and non-built-up as 61.93% and 38.07%, respectively. MNDWI shows that waterbodies cover nearly 1%, and BSI shows that bare soil or open areas cover 11.4%.

Land use at micro levels

LU at micro levels is assessed using Sentinal data (10 m resolution) through a supervised non-parametric classifier based on the Random Forest algorithm, which is presented in Supplementary Figure S4 (Figure S4a). Land use is classified into four classes: Built-up, vegetation, water, and barren (bare soil). Landsat data (with thermal band) used for urban heat island assessment is 30 m, while LU is assessed using Sentinal data of 10 m resolution. Nine pixels of LU (based on Sentinal data of 10 m spatial resolution) correspond to a pixel of Landsat thermal data, which aided in assessing the proportion of LU per pixel of Landsat data. The proportion of LU (at 10 m x 10 m, Sentinel) is further grouped into 12 classes (categories), which are labeled as C1, C2 …, and C12 and are presented in Supplementary Figure S4 (Figure S4b).

Supplementary Table S2 lists the proportion of LU (10 m resolution) corresponding to a pixel of 30 m resolution. The classes with the largest spatial extent include class 2 (C2, 37%), class 4 (C4, 14.75%), and fully vegetated class 11 (C11, 11.18%), followed by C3 (9.68%), C9 (6.7%), and C5 (4.67%). Class 12 (C12), consisting of only water, covers 0.95% of the area.

Land surface temperature

LST of Bengaluru city is estimated using the Landsat TIR data (30 m x 30 m) and is depicted spatially in (Fig. 3a), highlighting the prevalence of higher LST (red patches) in the southeast and northern portions of the city. The highest and lowest LST are 48 °C and 29.86 °C, respectively, with a mean temperature of 38.61 °C.

UTFVI analysis

Urban thermal field variance index (UTFVI) quantitatively evaluates the well-being of the environment concerning ecological thermal comfort while considering the UHI effect. The weak, normal, and middle UHI conditions are considered favorable ecological conditions, while the strong, stronger, and strongest are classified

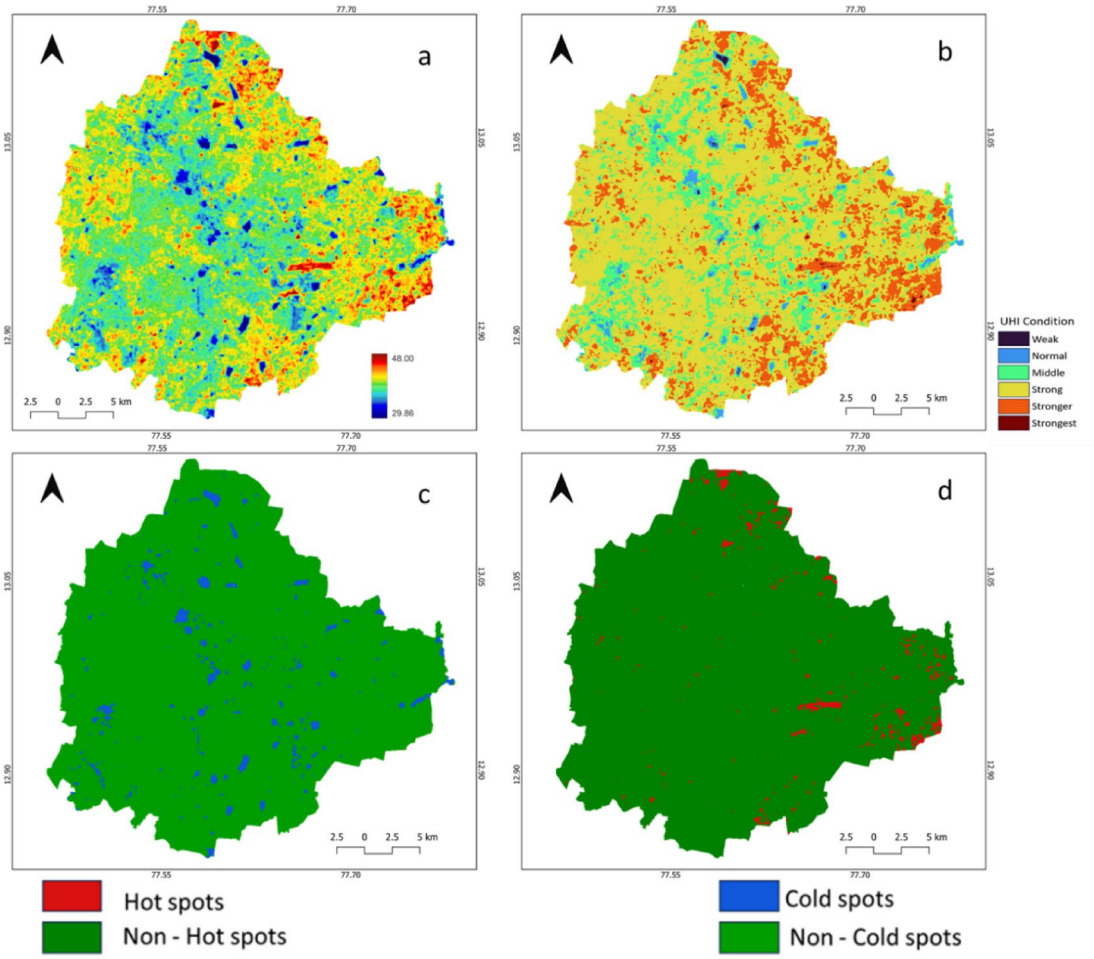

Fig. 3. (**a**) Estimated land surface temperature image from Landsat – 8 data, (**b**) UTFVI distribution map, (**c**) Urban cold spots, and (**d**) Cold hot areas. Created using the open-source software QGIS 3.22 [https://www.qgis.org/] and GRASS GIS 7.8.2 [https://wgbis.ces.iisc.ac.in/grass/].

as unfavorable. The area under favorable conditions was 168.93 km^2, whereas under unfavorable ecological conditions was 545.25 km^2. Figure 3b illustrates UHI conditions and the prevalence of UHI (545.25 sq. km) with poor ecological conditions.

Hot and cold spots analysis

LST values greater and less than the threshold values are termed UHI-affected areas and heat sinks. The threshold values for hot and cold spots were 44.53 and 35.08 °C, respectively. The distribution of urban cold and hot spots based on LST is given in (Fig. 3c,d), respectively. The area affected by high heat intensity is 15.41 km^2, and the heat sinks cover 23.85 km^2 of the city. The urban heat island phenomenon, when the areas affected are sparsely scattered, is known as the urban heat archipelago[15,19], which is illustrated in (Fig. 3d). A cluster of urban heat islands within a city/region is called an urban heat archipelago[15], representing the combined effect of multiple localized heat islands, forming a broader area of elevated temperatures. Figure 3d illustrates the same phenomenon, especially in the eastern and northern parts of the city, where various UHIs combine their effect to make heat archipelagos.

Land surface temperature of land use classes

Statistical analyses of temporal data of LST and LU (varied proportions) were carried out, and Fig. 4 illustrates LST variability (minimum, mean, and maximum) for different proportions of LU. Classes consisting of predominantly barren and urban classes showed the highest mean LSTs, specifically, class 1 (C1) consisting of entirely bare soil (39.92 °C), class 2 (C2) composed of entirely urban (39.74 °C), class 3 (C3, 39.57 °C), and class 4 (C4, 39.42 °C). Classes with mixed proportions of urban, barren, and vegetation (class C5-C10) and a minimal proportion of urban class showed a lower mean temperature. Class 5 (38.6 °C) and class 6 (38.37 °C) had high proportions of urban and barren areas, and they were warmer among the classes with mixed proportions of barren, vegetation, and urban areas. A gradual decrease in mean temperature can be seen as the urban proportion decreased in each class from class 6 (C6) onwards, class 7 (C7, with a mean temperature of 38.22 °C), class 8 (C8, 38.04 °C), class 9 (C9, 37.78 °C), and class 10 (C10, 37.56 °C). The water and vegetation classes showed the lowest mean LST,

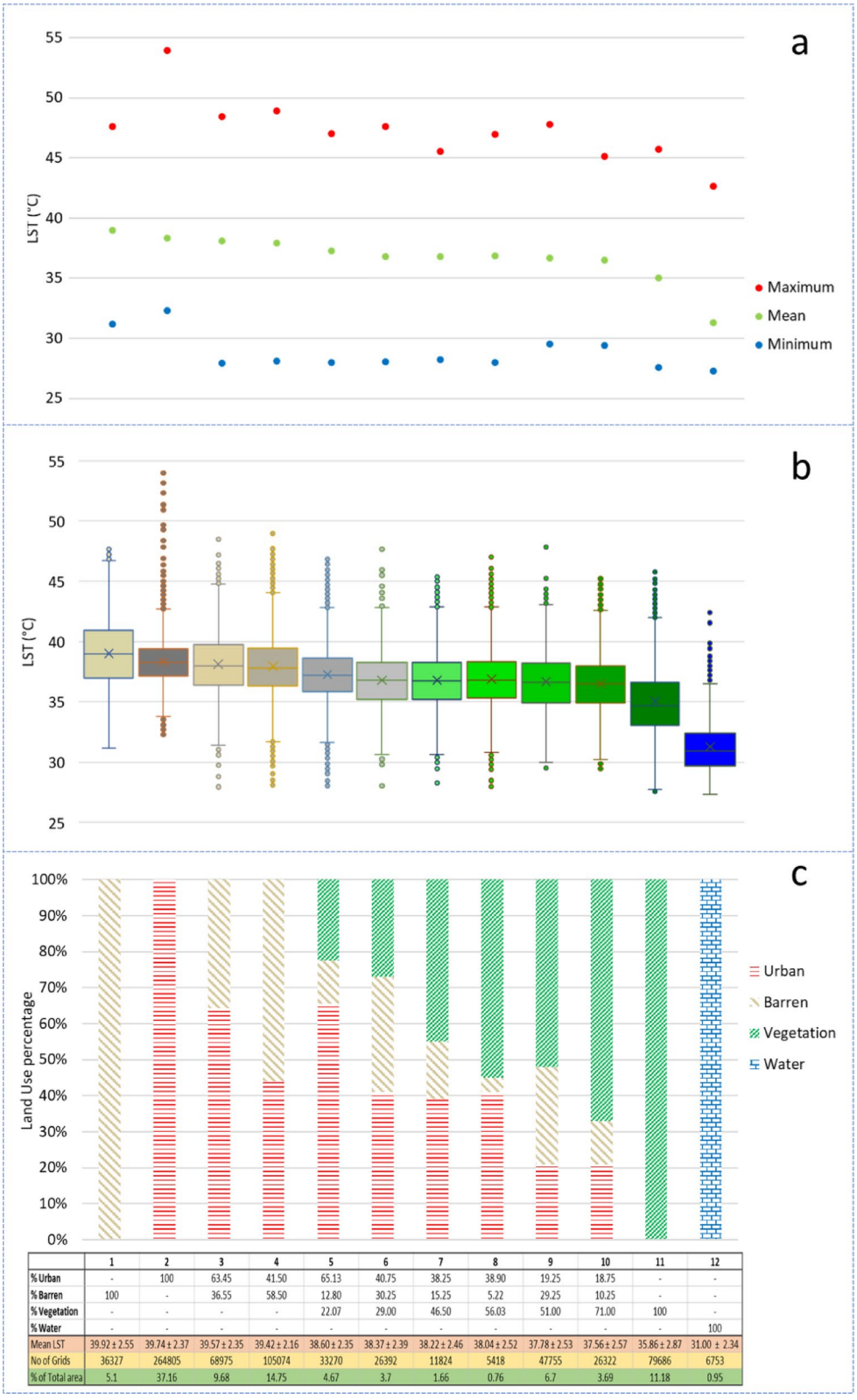

	1	2	3	4	5	6	7	8	9	10	11	12
% Urban	-	100	63.45	41.50	65.13	40.75	38.25	38.90	19.25	18.75	-	-
% Barren	100	-	36.55	58.50	12.80	30.25	15.25	5.22	29.25	10.25	-	-
% Vegetation	-	-	-	-	22.07	29.00	46.50	56.03	51.00	71.00	100	-
% Water	-	-	-	-	-	-	-	-	-	-	-	100
Mean LST	39.92 ± 2.55	39.74 ± 2.37	39.57 ± 2.35	39.42 ± 2.16	38.60 ± 2.35	38.37 ± 2.39	38.22 ± 2.46	38.04 ± 2.52	37.78 ± 2.53	37.56 ± 2.57	35.86 ± 2.87	31.00 ± 2.34
No of Grids	36327	264805	68975	105074	33270	26392	11824	5418	47755	26322	79686	6753
% of Total area	5.1	37.16	9.68	14.75	4.67	3.7	1.66	0.76	6.7	3.69	11.18	0.95

Fig. 4. (**a**) Variability of Land Surface Temperature - Minimum, mean, and maximum, (**b**) LST Variability assessment using Wiskar plot (box plot), (**c**) proportion of LU (computed considering Sentinel data of 10 m) in a pixel corresponding to LST (30 m resolution). Created using the open-source software QGIS 3.22 [https://www.qgis.org/] and Open Office 365.

with class 12 (C12) being the lowest (31.00 °C), followed by class 11 (C11, 35.86 °C). The decreasing LST with increasing vegetation cover highlights the role of vegetation as a heat sink and moderate microclimate: C7, C8, and C9 show nearly the same temperature. C8 exhibits a slightly elevated temperature compared to C9 due to its greater urban coverage. C12, characterized by water coverage, exhibits the lowest LST, indicating that areas near water bodies maintain lower temperatures than surrounding regions due to the heat modulation effects of evaporation. The current investigation of UHI with LU at the micro-level (proportion-based analysis) is a novel approach and contributes significantly to the UHI research domain and policy advocacy.

LST response to land cover (based on spectral indices)

Bivariate regression analyses reveal that the NDVI and MNDWI negatively correlate 0.46 and 0.23 with LST ($p < 0.00$), indicating that landscapes covered with vegetation and water bodies act as heat sinks. Similarly, the assessment of BSI and NDBI with LST showed a moderate positive correlation of 0.65 and 0.69, respectively ($p < 0.001$). Figure 5 depicts LST responses to various land cover indices -NDVI, MNDWI, BSI, and NDBI. The results indicate a lower variability of LST for water and vegetation compared to built-up and bare lands.

Multiple regression analyses of LST with the land cover types and the probable relationship is given in Eq. (3) with R^2 of 0.49 (with a standard error of 1.66).

$$\mathrm{LST} = 38.16 + 2.54 * (\mathrm{NDBI}) - 5.36 * (\mathrm{NDVI}) - 8.60 * (\mathrm{MNDWI}) + 6.73 * (\mathrm{BSI}) \quad (3)$$

Equation 3 highlights that the increment of NDBI by 0.1 would enhance LST by 0.25 °C. Similarly, BSI changing by 0.1 would increase LST by 0.67 °C. In the NDVI and MNDWI (representing vegetation and waterbodies), an increment of 0.1 of NDVI and MNDWI would reduce LST by 0.53 and 0.86 °C, respectively.

Discussion

The Comprehensive Development Plan (CDP) for Bangalore (approved by the Government of Karnataka) has been developed by the Bangalore Development Authority, which is the Planning Authority for the Metropolitan area of Bangalore, as required under Sect. 25 of the Karnataka Town & Country Planning Act 1961[40]. The Master Plan was prepared under Sect. 9 of the Karnataka Town and Country Planning Act 1961 (KTCP Act, 1961) and has been revised once every ten years as per Section 13D of the KTCP Act, 1961[40]. The Master Plan for BMA (i.e., RMP 2015), prepared and approved on June 25, 2007, is currently in force, which aims to guide urban development, including a defined conurbation area and areas designated for green belts and agricultural land. The plan aimed to achieve a compact, balanced, and equitable urban growth for the city[41]. RMP 2015 advocated mitigation of uncontrolled sprawl by strengthening existing urban patterns and proposed zoning and land use regulations to designate areas for specific purposes, ensuring a well-organized cityscape[41,42]. However, the city landscape witnessed rapid urbanization during the past two decades, consequent to globalization and the relaxation of markets (https://wgbis.ces.iisc.ac.in/sdss/BUiS/).

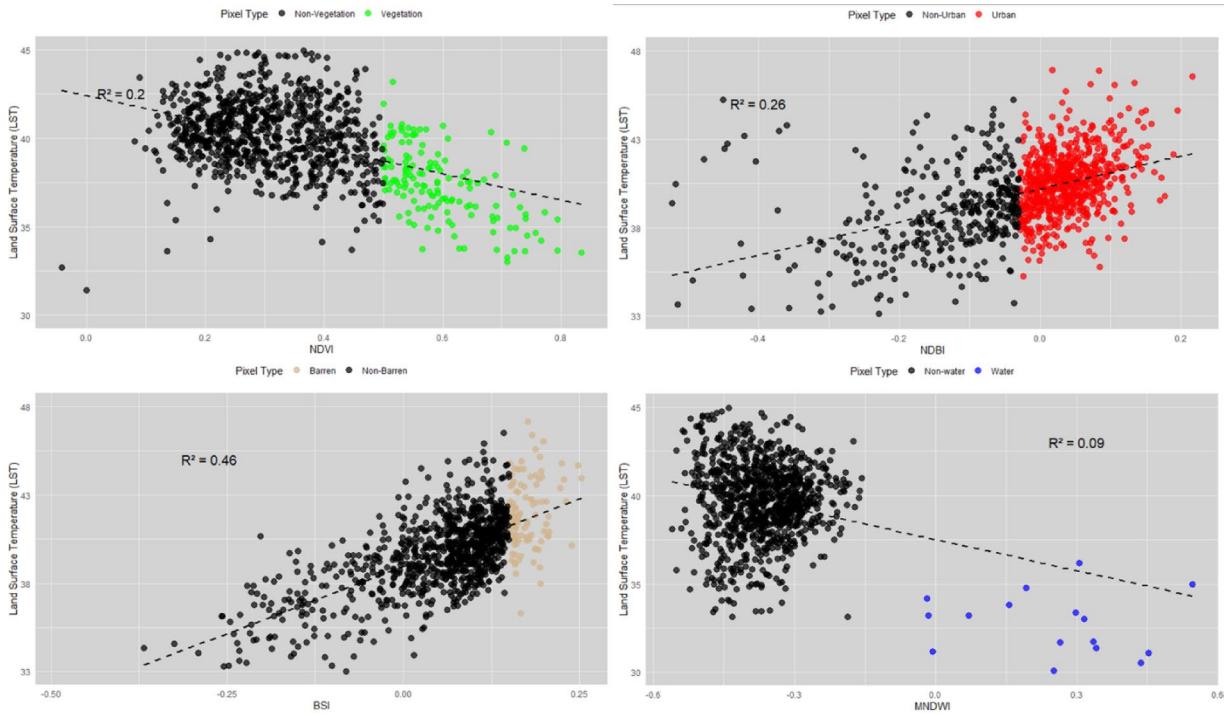

Fig. 5. LST responses to land cover (computed through spectral indices). The X axis is a spectral index, and the Y is LST in °C. Created using open-source statistical software (R).

Figure 6 depicts the temporal changes in the number of lakes in Bangalore from 1973 to 2023. The city landscape had 756 lakes (in 1973), which is reduced to 216 (2023), which is mainly due to intense urbanization and urban sprawl (https://wgbis.ces.iisc.ac.in/sdss/BLIS/). Field survey reveals that lakes (98%) are encroached on by illegal buildings (high-rise apartments, commercial buildings, slums, etc.), nearly 90% of lakes are sewage-fed, slums surround 38% of lakes, and 82% of lakes show a sharp decline in vegetation cover in the catchment[43]. Multi-story buildings have come up in many lake beds, and stormwater drains hinder the natural catchment flow[43]. The decline in wetlands is correlated with the increase in built-up area due to the concentrated growth model adopted by the state executive system, which severely affected open spaces, particularly water bodies[44]. Temporal land use analyses for Bangalore City, India, reveal the transition of a porous landscape (with >68% vegetation cover and water bodies in 1973) to a paved landscape (87%) with minimal vegetation cover. These LU changes lead to changes in the surface properties of a landscape that control the exchange of energy between the land surface and the atmosphere, which alters surface energy balance (SEB), resulting in LST changes. Responses of LST to LU changes have been explored to understand linkages, which would provide invaluable insights into landscape planning and the prudent management of ecosystems[44,45].

Temporal ambient air temperature details complied from the India Meteorological Department (https://mausam.imd.gov.in/) monitoring stations in Bangalore reveal that ambient temperature has shown an increasing trend with the alteration in landscape structure with an increase in paved surfaces (buildings, roads, etc.) and decline of natural porous surfaces (vegetation, lakes, etc.): 16 °C (Paved surfaces: 1.14%, Porous surfaces: 98.22%), to 18 °C (Paved surfaces: 7.97%, Porous surfaces: 92.03%), 19 °C (Paved surfaces: 27.3%, Porous surfaces: 72.7%), 21 °C (Paved surfaces: 37.4%, Porous surfaces: 62.26%), 28 °C (Paved surfaces: 54.42%, Porous surfaces: 45.58%) and 34 °C (Paved surfaces: 87.65%, Porous surfaces: 12.36%), which conform to LST dynamics with alteration in urban morphology (Figs. 3 and 4). Figure 7 illustrates an upward trend in ambient air temperature with increased paved surfaces and decreased porous surfaces.

The current LU of Bangalore highlights the dominance of urban (class C2), followed by class 4 (C4, consisting of 41.50% urban and 58.50% barren area), and sparse class 11 (C11, containing only vegetation). LST analysis shows that the city has a mean LST of 38.61 °C, and thresholds of LST for hot and cold spots are 44.53 °C and 35.08 °C, respectively. The area influenced by high heat intensity is 15.41 km^2, while heat sinks cover 23.85 km^2 of the city. The UTFVI analysis shows that 76% of the city areas with unfavorable ecological conditions experience enhanced thermal discomfort, necessitating immediate mitigation measures through improved green spaces and rejuvenation of water bodies (lakes)[46,47].

The UHI also depends on the complex interplay of confounding variables, such as terrain elevation, atmospheric circulation (wind direction and speed), and proximity to waterbodies that significantly influence local temperature dynamics. The elevation reduces the temperature due to the lapse rate, and waterbodies modulate heat through evaporation. The topography of Bangalore is flat terrain, and hence, the role of topography in UHI is minimal.

The evaluation of the effect of LU on LST reveals that green cover or vegetation cover and water bodies in the landscape aid as heat sinks, lowering LST. Barren areas and urban pockets (paved surfaces) had the higher LST among all classes. The spatial extent of individual housing plots in Bengaluru is nearly 900 m^2, equivalent to a pixel of TIR (Landsat) and derived LST pixel. Land use composition in this pixel was assessed using 10 × 10 m Sentinel data, providing insights into the thermal comfort of the residential plot or industrial work area. Evaluation of LST with LU composition in a pixel reveals that attaining the desired thermal comfort plot requires relatively higher vegetation cover with urban (C9 and C10). The LST of C9 and C10 is relatively lower than other micro-level land use classes and has the desired thermal comfort. However, considering socio-economic aspects,

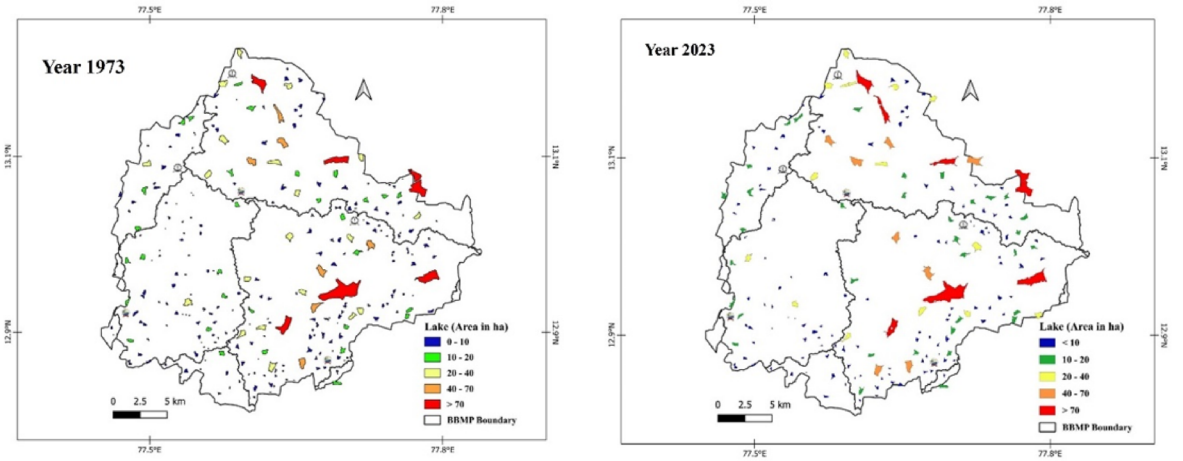

(a) Spatial distribution of lakes in 1973 (as per the Survey of India topographic maps)

(b) Spatial distribution of lakes (2023) based on the field survey

Fig. 6. Spatial distribution of lakes – (**a**) 756 (in 1973) and (**b**) 216 (in 2023).

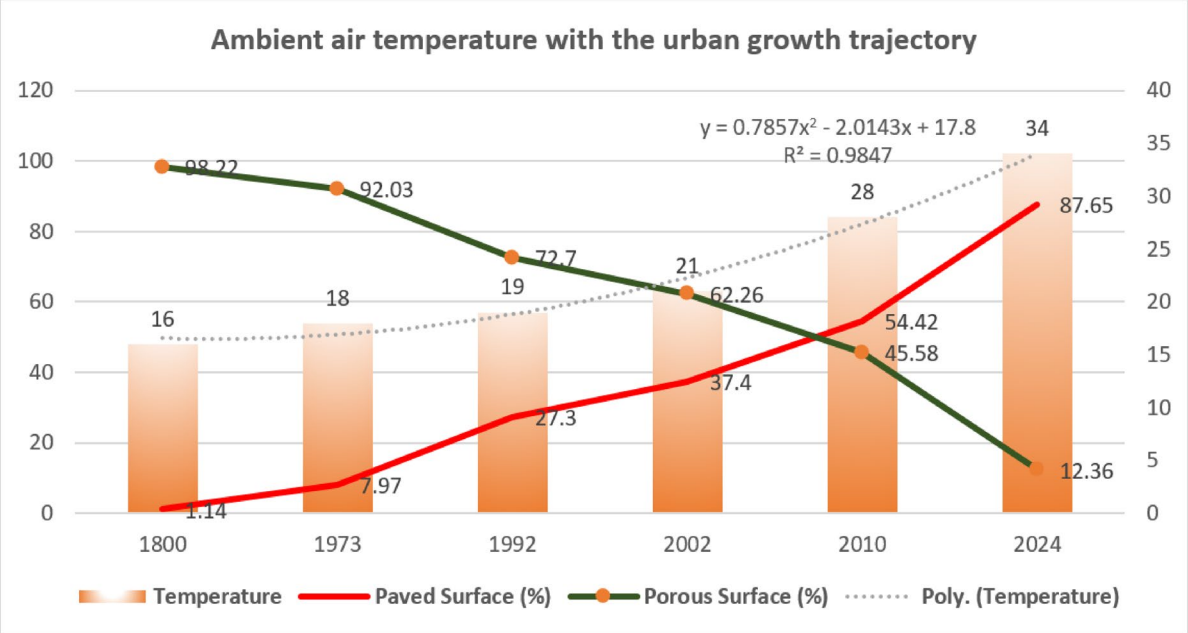

Fig. 7. Ambient air temperature in Bangalore with urban morphology (% changes in paved surfaces and porous surfaces).

at least 30% of vegetation (C6) must be maintained in a region to attain the desired thermal comfort, which helps balance urban growth with ecological, hydrological, environmental, and economic sustainability.

NDBI and BSI are positively correlated with LST, confirming the role of the land surface in maintaining the surface energy balance (Fig. 5). On the contrary, NDVI and MNDWI negatively correlate with LST (Fig. 5), highlighting micro-climate moderation services by ecosystems such as vegetation and water bodies. Multiple linear analysis shows that paved surfaces (built-up, etc.) and bare soil areas strongly affect LST, while porous surfaces (vegetation and water bodies) showed a moderate effect on LST.

The spatial analyses of LST with LU provide insights to mitigate the Urban Heat Island (UHI) effect and optimize the favorable land use composition to optimize thermal comfort in densely populated cities like Bangalore. This entails securing the remaining patches of urban forests in the city and removing encroachment from the protected and reserved forests (including National Parks), and Thippgondanahalli Reservoir – Arkavati river systems are eco-sensitive zones[41,42]. Lakes and valley systems are environmentally essential resources to be prudently managed to maintain micro climate as valleys aid in trapping warm air during the day and allow cold air to drain at night, potentially leading to localized cooler temperatures[43]. Lakes play a significant role in regulating UHI due to the cooling effect through evaporation[47].

Policy recommendations to mitigate UHI in cities are (i) increase and protect green spaces for enhancing urban environment quality and mitigate the impact of urbanization[2,13], (ii) integrate green infrastructure into urban development plans, protect existing trees, and promoting sustainable urban landscaping[45,47], (iii) a mini forest of native species in each ward to moderate local temperature[47], (iv) maintaining 30% open spaces with green cover at plot levels (C6) for a desired thermal comfort, (v) connecting fragmented tree patches for promotion of ecosystem health and sustainability[48]. (v) rejuvenating lakes (there are 216 lakes in 198 municipality wards) to retain rainwater and facilitate groundwater recharge, which helps in moderating micro climate[44], (vi) decentralized governance involving local stakeholders for prudent management of common lands (lakes, parks, open spaces), (vii) mandatory UHI mitigation measures at local levels through green roofs, and walls that cool buildings by shading and evapotranspiration, reflecting materials, etc., (viii) developing green lanes through planting native tree species on either side of lanes, and (ix) ensure self-governance (decentralized governance) and strengthening local institutions as per Nagarpalika Act[49].

Stakeholder meeting

Discussion with Dr. Sunil Kumar, Chief Town Planner at the Directorate of Town and Country Planning (http://www.dtcp.gov.in/en) after a preliminary analysis of LST with landscape dynamics in Bangalore led to a request for analyses at a micro level (or plot level) to recommend appropriate building regulation such as the imposition of conditions and restrictions concerning the open space in a plot, the percentage of building area for a plot, the number, size of the building, building height, floor area ratio, etc. to enhance the thermal comfort.

A discussion meeting to apprise of the outcome of the micro-level analyses (at plot level) and policy recommendation of maintaining 30% open space with green cover at plot level to enhance thermal comfort at individual houses was organised with the stakeholders involving Chief Town Planner, Directorate of Town and Country Planning (http://www.dtcp.gov.in/en) and select representatives of non-governmental organizations and residents on June 5 2025 at CES TE15, Energy & Wetlands Research Group, Indian Institute of Science,

Bangalore 560,012. The meeting was fruitful as all participants concurred with the policy recommendations, and the chief town planning officer assured them that the outcome of the current research would be incorporated with recommendations in the proposed Master plan 2031[50].

Limitations of the current study and scope for further research

The current research provides insights into urban planning to enhance thermal comfort by mitigating UHI. However, the current work has certain limitations that provide opportunities for further research. The current study focuses on land surface temperatures (LST) for mapping UHI. The research may serve as a foundation for subsequent micro-level proportion-based investigations. Advancements in geospatial technology enable the utilization of higher-resolution land surface temperature and optical data for more detailed micro-studies.

The lack of in-situ data for validation of the LST is a major limitation, as we can not validate the LST with the acquisition of imagery. Additionally, the use of single-date imagery, a major limitation of the study, comes with an inability to capture temporal variations.

Considering LST and air temperature with other subtle factors is required to understand UHI dynamics comprehensively. Moreover, investigations of UHI intensities with economic and health aspects would unravel the complex relationships of unplanned urbanization with economic status and UHI effects. Many cities in India and tropical regions experienced heatwaves with increased temperatures for prolonged periods, necessitating consideration of the duration and intensity of heat waves with the escalation of UHI, particularly in scenarios where temperatures exceed dangerous thresholds for prolonged periods. The method adopted for mapping UHI at the micro level is replicable to any region across the tropical and sub-tropical climate zones. The current protocol serves as a foundation for subsequent micro-level UHI investigations. Advancements in geospatial technology with improvements in space-borne sensors (thermal, optical, and microwave) would give impetus to detailed micro-level studies for designing sustainable, liveable cities by maximizing socio-economic benefits while ensuring health.

Materials and methods

Study area: Bangalore city, Karnataka state, India

The city of Bangalore (or Bengaluru) is the principal administrative, cultural, commercial, industrial, and knowledge capital of the state of Karnataka, India, with a spatial extent of 741 km^2 and located between 12°39'00" to 13°13'00"N and 77°22'00" to 77°52'00"E, in the southeastern part of Karnataka, India[13], within the Bengaluru Urban district and in the Mysore plateau at a mean elevation of 720 m (Fig. 8) above mean sea level. The elevated position gives the city a moderate climate, and the city has the distinction of having a pleasant and salubrious climate throughout the year. The terrain around Bengaluru is characterized by rolling hills, rocky outcrops, and lush greenery, particularly on the outskirts. While the city is relatively flat, the surrounding landscape includes small hills and valleys, especially in areas like the Nandi Hills to the north, a prominent feature of the region's topography[2]. The city's varied elevation adds to its scenic beauty, with lakes, and parks dot the landscape. The city witnessed rapid urbanization and consequent urban growth with intense urbanization. Urban sprawl is a local phenomenon in peri-urban areas along ring roads, highways, and around service facilities, eventually becoming the urban centre hub and extending in all directions[13]. The city is identified as the *'Silicon Valley'* of India and has emerged as one of the technological innovation hubs.

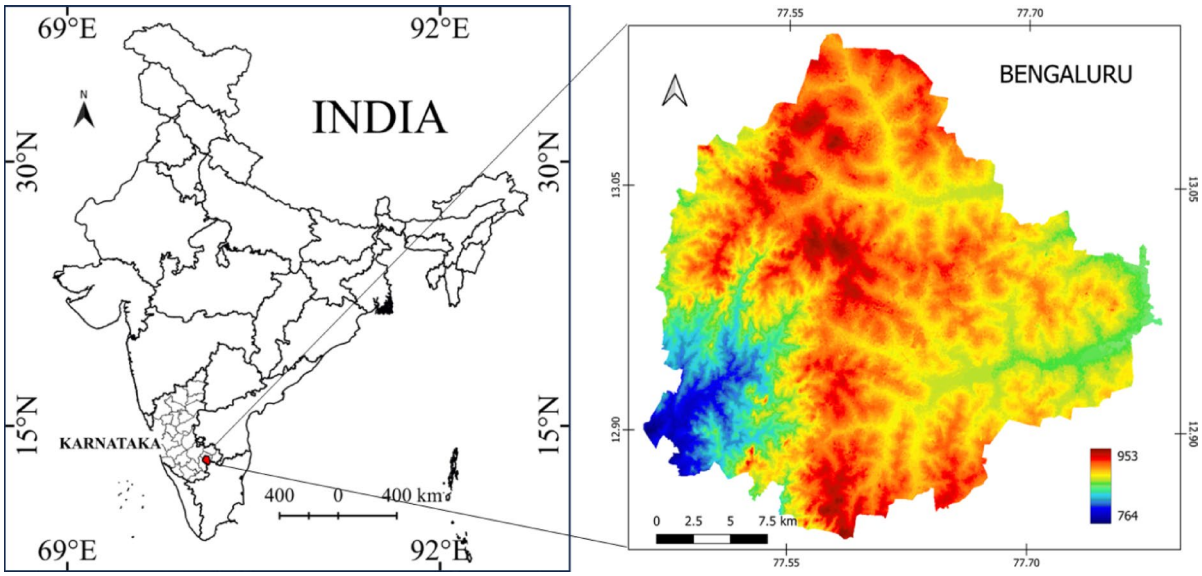

Fig. 8. Bengaluru city (with the elevation profile), Karnataka State, India. Created using the open-source software QGIS 3.22 [https://www.qgis.org/] and GRASS GIS 7.8.2 [https://wgbis.ces.iisc.ac.in/grass/].

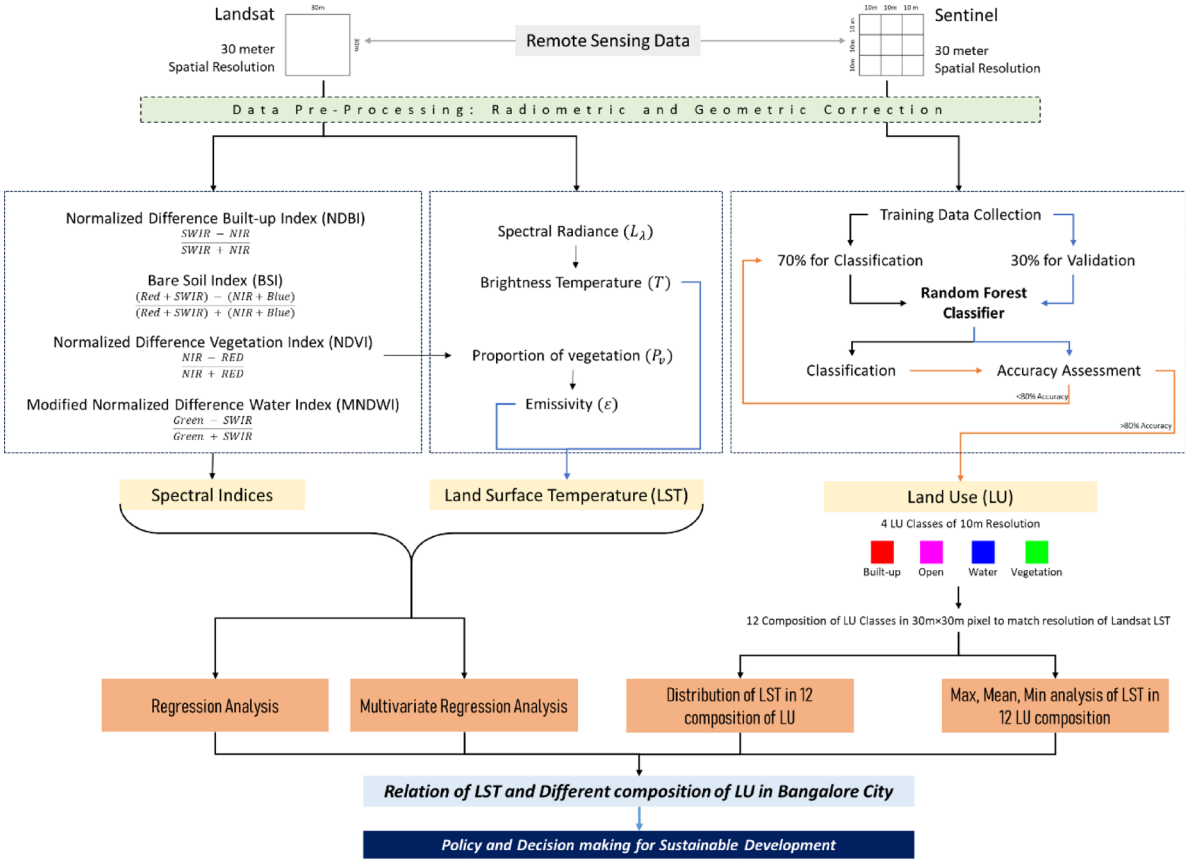

Fig. 9. The method adopted for estimating LST and LU dynamics.

Method

Figure 9 outlines the method adopted for estimating LST and land use dynamics using the temporal remote sensing data - Landsat 8 and Sentinel 2, with spatial resolution of 30 m and 10 m, respectively. Land use, land cover, and land surface temperature were estimated using Google Earth Engine(https://earthengine.google.com), open-source software QGIS 3.22 [https://www.qgis.org/] and GRASS GIS 7.8.2 [https://wgbis.ces.iisc.ac.in/grass/].

The datasets (Landsat and Sentinel data) were chosen to ensure minimal cloud coverage (< 5%) of April 2022. The Landsat thermal data has a spatial resolution of 30 m and an area corresponding to 900 m2 per pixel[38], and Sentinel-2 has a spatial resolution of 10 m and an area corresponding to 100 m^2 per pixel[39]. A pixel of Landsat (thermal data) corresponds to 9 pixels of Sentinel-2 data (optical data). The data were pre-processed to rectify geometrical and radiometric discrepancies in the Google Earth Engine (GEE) Platform (https://earthengine.google.com/). All these spatial data corresponding to the study area were reprojected to a common geodetic datum, the World Geodetic System 1984 (WGS84), and Universal Transverse Mercator (UTM) within 43 N zones, ensuring consistency in mapping. Road networks were extracted from Survey of India topographic maps at scales of 1:50,000 and 1:250,000 (https://www.surveyofindia.gov.in). The city administrative boundary maps were acquired from the K-GIS portal (https://kgis.gok.in). Training data corresponding to LU categories for LU classification were gathered from various locations within the study area using a handheld pre-calibrated global positioning system (GPS), and online spatial portals (Google Earth - https://earth.google.com), and Bhuvan (https://bhuvan.nrsc.gov.in) with high-resolution remote sensing data. The study considered Virtual spatial maps such as Bhuvan (http://bhuvan.nrsc.gov.in) and high-resolution Google Earth (http://earth.google.com) to validate classified thematic maps.

Assessment of land cover

Land cover assessment is done through spectral indices such as normalized difference vegetation index (NDVI) to delineate the spatial extent of vegetation and non-vegetation considering NIR and Red bands as per Eq. (4).

The spatial extent of the built-up area is acquired through normalized difference built-up index (NDBI), calculated with SWIR and NIR bands (as per Eq. 5). Similarly, the spatial extent of waterbodies and bare soil is calculated with modified normalized difference water index (MNDWI) and normalized difference bare soil index (NDBSI). MNDWI is calculated using Green and SWIR bands Eq. (6), whereas NDBSI is calculated using SWIR, NIR, Red, and Blue bands Eq. (7).

$$NDVI = \frac{NIR-R}{NIR+R} \tag{4}$$

$$NDBI = \frac{SWIR-NIR}{SWIR+NIR} \tag{5}$$

$$MNDWI = \frac{GREEN-SWIR}{GREEN+SWIR} \tag{6}$$

$$NDBSI = \frac{(RED+SWIR)-(NIR+BLUE)}{(RED+SWIR)+(NIR+BLUE)} \tag{7}$$

NIR, RED, and SWIR are near-infrared, red, and short-wave infrared bands of the LANDSAT 8 satellite. Supplementary Table S3 lists spectral indices used for land cover analyses to delineate areas under vegetation, etc.

Assessment of land use dynamics

Temporal remote sensing data from 1973 to 2025 (downloaded from https://landsat.gsfc.nasa.gov/data/) were classified using a supervised classification technique based on a non-parametric algorithm - Random Forest (RF) through Google Earth Engine (an open-source cloud-based platform, https://earthengine.google.com).

LU analyses involve generating FCC (false color composites) from remotely acquired data bands (NIR, Red, and Green) to identify heterogeneous landscape patches. Training polygons were digitized from FCC corresponding to heterogeneous patches representing all LU classes, covering 15% of the study, and are uniformly distributed throughout the study area. The attribute information for these training polygons was collected from the field, using pre-calibrated handheld global positioning systems (GPS) and high spatial resolution data from Google Earth (https://earth.google.com). 70% of training polygons are used for supervised classification, while the remaining (30%) are used for testing[34,51]. Spatial data (RS) were classified using a supervised machine learning algorithm, Random Forest (RF). The classifier accuracy is evaluated through an error matrix by computing overall accuracy, producer accuracy, user accuracy, and kappa statistics, which provide impartial error estimates. Spatial statistics of land uses were generated using QGIS [https://www.qgis.org/] and GRASS [https://wgbis.ces.iisc.ac.in/grass/] and analyzed using Open Office 365.

RF is a novel technique that uses a set of decision trees selected randomly from the training set to aggregate decisions for determining the final class and provides a higher level of accuracy for land use classification in a diverse landscape. Each tree is constructed based on the randomly sampled feature vectors with replacement, independently generated with a uniform distribution shared across all decision trees to acquire high training data accuracy and enhance generalization accuracy as their complexity increases. These multiple classifiers are typically aggregated through bagging - a plurality voting scheme[52,53]. RF can effectively handle multi-dimensional data while employing a substantial number of trees within the ensemble[34,52]. Hyperparameter tweaking revealed that employing 100 decision trees produced the most optimal outcomes[54–56].

Assessment of LU (at micro levels) and LST

Remote sensing data (Sentinel data of 10 m x 10 m resolution) was classified to derive land uses using training data through a non-parametric supervised classifier Random Forest in Google Earth Engine (https://earthengine.google.com), LST is computed using thermal data of LANDSAT of 30 m x 30 m resolution. A pixel of LST corresponds to 9 LU pixels derived from Sentinel data (10 m x 10 m resolution). LU pixels were grouped based on the proportion of LU corresponding to a pixel of LST. Supplementary Table S2 provides 11 such groupings, which aided in exploring LST relationships with LU at micro levels.

Land surface temperature

Computation of LST using TIR (thermal) data of LANDSAT 8 as per Eqs. (8) and (9) involved (i) converting the pixel values to spectral radiance. (ii) computing the brightness temperature with spectral radiance. (iii) computation of NDVI to assess the proportion of vegetation. (iv) computation of emissivity[9,18,20,21].

$$LST = \frac{T}{1+\left(\lambda * \frac{T}{\rho}\right) * \log\epsilon} \tag{8}$$

$$where,\ \rho = \frac{h*c}{\sigma} \tag{9}$$

Where T is Brightness temperature; λ is wavelength of emitted radiation; ε is land surface emissivity; σ = Stefan Boltzmann's constant (5.67×10^{-8} $Wm^{-2}K^{-4}$ = 1.38×10^{-23} J/K), h = Planck's constant (6.626×10^{-34} Jsec), c = velocity of light (2.998×10^{8} m/sec), and ε is spectral emissivity[57].

Computation of spectral radiance using TIR pixel values (digital numbers)
Spectral radiance is computed as per Eq. (10).

$$L_\lambda = M_L \times Q_{Cal} + A_L \tag{10}$$

Where, where $L\lambda$ is the spectral radiance of the upper part of the atmosphere (TOA) expressed in W/ (m^2.sr.µm);

M_L is the specific multiplicative factor of the band, and A_L is the additive rescaling factor specific to the TIR band and A_L is the additive rescaling factor specific to the TIR band, (available in the metadata of the Landsat images) and *QCal* is the DN value of a pixel.

Calculating brightness temperature
The brightness temperature (in Celsius) is computed from spectral band radiance as per Eq. (11).

$$T = \left(\frac{K_2}{\log\left(\frac{K_1}{L_\lambda}\right)} \right) - 273.15 \tag{11}$$

Where $L\lambda$ is the spectral radiance derived from Eq. (7), and *K1* and *K2* are the thermal conversion constants of the TIR data (available in metadata).

Computation of the spatial extent of vegetation
The spatial extent of vegetation is computed through NDVI (normalized difference vegetation index), and the proportion of vegetation is calculated as per Eq. (12).

$$P_v = \left(\frac{NDVI - NDVI_{min}}{NDVI_{max} - NDVI_{min}} \right)^2 \tag{12}$$

Where *NDVImax* and *NDVImin* are the maximum and minimum values of NDVI.

Computation of emissivity
Land surface emissivity corresponding to LU type is computed as per Eq. (13).

$$\epsilon = 0.004 \times Pv + 0.986 \tag{13}$$

Probable relationship of LST with spectral indices

The probable relationship of LST with spectral indices is assessed through (a) bivariate and (b) multivariate regression analysis. Bivariate regression analysis was done to understand the interaction of different land covers typified by a spectral index with LST. One thousand points were taken randomly to analyze each regression between spectral indices and LST. Multivariate regression analysis was done considering all the variables to understand the factors responsible for variation in LST. Multivariate regression provides insights into the role of multiple variables in LST and is computed as per Eq. (14).

$$y = a_0 + a_1X_1 + a_2X_2 + a_3X_3 + a_4X_4 \tag{14}$$

Here, *y* is a dependent variable; *X1*, *X2*, *X3*, and *X4* are independent explanatory variables; *a1*, *a2*, *a3*, and *a4* are the coefficient of the corresponding explanatory variables that describe their influence factor; *a0* is the intercept of the equation[15].

Urban hotspots are locations with very high temperatures compared to the neighborhood and are uncomfortable for human activities[58]. Urban hot and cold spots are delineated using LST values in the study region shown in Eqs. (15) and (16), respectively.

$$LST > \mu + 2 * \sigma \tag{15}$$

$$LST < \mu + 2 * \sigma \tag{16}$$

Here, μ mean LST and σ standard deviation of LST.

Urban thermal field variance index (UTFVI)

Is computed considering LST and ambient temperature as per Eq. (17). Supplementary Table S4 lists the UTFVI threshold for the different UHI conditions.

$$UTFVI = \frac{LST - T_{mean}}{T_{mean}} \tag{17}$$

Here, T_{mean} is the mean temperature.

Data availability

Data are archived at our data portal: https://wgbis.ces.iisc.ac.in/sdss/BUiS/.

Received: 4 April 2025; Accepted: 25 June 2025
Published online: 08 July 2025

References

1. Mallik, R. et al. Spatio-temporal analysis of environmental criticality: Planned versus unplanned urbanization. In *IOP Conference Series: Earth and Environmental Science* **1164** (1), 012014 https://doi.org/10.1088/1755-1315/1164/1/012014 (IOP Publishing, 2023).
2. Ramachandra, T. V., Aithal, B. H. & Sanna, D. D. Insights to urban dynamics through landscape Spatial pattern analysis. *Int. J. Appl. Earth Obs. Geoinf.* **18**, 329–343. https://doi.org/10.1016/j.jag.2012.03.005 (2012).
3. Gupta, N. & Aithal, B. H. Urban land surface temperature forecasting: a data-driven approach using regression and neural network models. *Geocarto Int.* **39** (1), 2299145. https://doi.org/10.1080/10106049.2023.2299145 (2024).
4. UN DESA. 2018 Revision of world urbanization prospects. (accessed 5 March 2025); https://population.un.org/wup/Publications/Files/WUP2018-Report.pdf

5. Simon, E. B., John, K. & Mattias, K. Compact city planning and development: Emerging practices and strategies for achieving the goals of sustainability, *Dev. Built Environ.* **4**, 100021 https://doi.org/10.1016/j.dibe.2020.100021 (2020).
6. Ronita, B., Kiyo, K. & Keisuke, H. Does compact urban forms relate to good quality of life in high density cities of india?? Case of kolkata, cities. **48**, 55–65 https://doi.org/10.1016/j.cities.2015.06.005 (2015).
7. Randal, O. How urban planners cause the housing bubble, Cato Institute Policy Analysis. (accessed 5 June 2025); https://ciaotest.cc.columbia.edu/wps/cato/0017623/f_0017623_15101.pdf
8. Randal, O. The myth of the compact city, - why compact development is not the way to reduce carbon dioxide emissions, Cato Institute Policy Analysis. https://www.cato.org/sites/cato.org/files/pubs/pdf/pa653.pdf (2009).
9. Aires, F., Prigent, C., Rossow, W. B. & Rothstein, M. A new neural network approach including first guess for retrieval of atmospheric water vapor, cloud liquid water path, surface temperature, and emissivities over land from satellite microwave observations. *J. Geophys. Research: Atmos.* **106** (D14), 14887–14907. https://doi.org/10.1029/2001JD900085 (2001).
10. Sun, D. & Pinker, R. T. Estimation of land surface temperature from a geostationary operational environmental satellite (GOES-8). *J. Geophys. Research: Atmos.* **108** (D11). https://doi.org/10.1029/2002JD002422 (2003).
11. Malik, M. S. & Shukla, J. P. Retrieving of land surface temperature using thermal remote sensing and GIS techniques in Kandaihimmat watershed, hoshangabad, Madhya Pradesh. *J. Geol. Soc. India*. **92** (3), 298–304. https://doi.org/10.1007/s12594-018-1010-y (2018).
12. Sahani, N. Assessment of spatio-temporal changes of land surface temperature (LST) in Kanchenjunga biosphere reserve (KBR), India using Landsat satellite image and single channel algorithm. *Remote Sens. Applications: Soc. Environ.* **24**, 100659. https://doi.org/10.1016/j.rsase.2021.100659 (2021).
13. Ramachandra, T. V. & Kumar, U. Greater bangalore: emerging urban heat Island. *GIS Dev.* **14** (1), 86–104 (2010). https://wgbis.ces.iisc.ac.in/energy/paper/Bangalore_heatisland/IISc_TVR_UK_Bangalore_Urban_Heat191209.pdf
14. Moazzam, M. F. U., Doh, Y. H. & Lee, B. G. Impact of urbanization on land surface temperature and surface urban heat Island using optical remote sensing data: A case study of Jeju island, Republic of Korea. *Build. Environ.* **222**, 109368. https://doi.org/10.1016/j.buildenv.2022.109368 (2022).
15. Yuan, Y. et al. Surface urban heat island effects intensify more rapidly in lower income countries. *npj Urban Sustain.* **5**, 11 https://doi.org/10.1038/s42949-025-00198-9 (2025).
16. Liu, Z. et al. Surface warming in global cities is substantially more rapid than in rural background areas. *Commun. Earth Environ.* **3**, 219. https://doi.org/10.1038/s43247-022-00539-x (2022).
17. Oke, T. R. The energetic basis of the urban heat Island. *Q. J. R Meteorol. Soc.* **108**, 1–24. https://doi.org/10.1002/qj.49710845502 (1982).
18. Arnfield, A. J. Two decades of urban climate research: a review of turbulence, exchanges of energy and water, and the urban heat Island. *Int. J. Climatol.* **23**, 1–26. https://doi.org/10.1002/joc.859 (2003).
19. Alizadeh, M. R. et al. Increasing heat-stress inequality in a warming climate. *Earth's Future*. **10**, e2021EF002488. https://doi.org/10.1029/2021EF002488 (2022).
20. Feng, R., Wang, F., Wang, K., Wang, H. & Li, L. Urban ecological land and natural-anthropogenic environment interactively drive surface urban heat island: An urban agglomeration-level study in China. *Environ. Int.* **2021** (157), 106857 https://doi.org/10.1016/j.envint.2021.106857 (2021).
21. Yu, Z., Yao, Y., Yang, G., Wang, X. & Vejre, H. Strong contribution of rapid urbanization and urban agglomeration development to regional thermal environment dynamics and evolution. *For. Ecol. Manag.* **446**, 214–225. https://doi.org/10.1016/j.foreco.2019.05.046 (2019).
22. Li, Y., Sun, Y. W., Li, J. L. & Gao, C. Socio-economic drivers of urban heat island effect: Empirical evidence from major Chinese cities. *Sustain. Cities Soc.* **63**, 102425 https://doi.org/10.1016/j.scs.2020.102425 (2020).
23. Newman, M. The compact City fallacy. *J. Plann. Educ. Res.* **25**, 11–26. https://doi.org/10.1177/0739456X04270466 (2005).
24. Yang, C. et al. Associations of compound hot extremes and heat waves with first-ever stroke morbidity in the context of climate change. *Adv. Climate Change Res.* **16** (2), 425–432 https://doi.org/10.1016/j.accre.2025.03.012 (2025).
25. Jain, S. et al. Urban heat Island intensity and its mitigation strategies in the fast-growing urban area. *J. Urban Manag.* **2020** (9), 54–66. https://doi.org/10.1016/j.jum.2019.09.004 (2020).
26. Ramachandra, T. V. et al. Insights into the linkages of forest structure dynamics with ecosystem services. *Sci. Rep.* **15**, 15606. https://doi.org/10.1038/s41598-025-00167-3 (2025).
27. Hong, T. & Heo, Y. Exploring the impact of urban factors on land surface temperature and outdoor air temperature: A case study in seoul, Korea. *Build. Environ.* **243**, 110645. https://doi.org/10.1016/j.buildenv.2023.110645 (2023).
28. Haldar, S., Mandal, S., Bhattacharya, S. & Paul, S. Dynamicity of land use/land cover (LULC) an analysis from peri-urban and rural neighbourhoods of Durgapur municipal corporation (DMC) in India. *Reg. Sustain.* **4** (2), 150–172. https://doi.org/10.1016/j.regsus.2023.05.001 (2023).
29. Ezimand, K., Azadbakht, M. & Aghighi, H. Analyzing the effects of 2D and 3D urban structures on LST changes using remotely sensed data. *Sustainable Cities Soc.* **74**, 103216. https://doi.org/10.1016/j.scs.2021.103216 (2021).
30. Han, W. Analyzing the scale dependent effect of urban Building morphology on land surface temperature using random forest algorithm. *Sci. Rep.* **13** (1), 19312. https://doi.org/10.1038/s41598-023-46437-w (2023).
31. Abir, F. A., Ahmmed, S., Sarker, S. H. & Fahim, A. U. Thermal and ecological assessment based on land surface temperature and quantifying multivariate controlling factors in bogura, Bangladesh. *Heliyon* **7** (9). https://doi.org/10.1016/j.heliyon.2021.e08012 (2021).
32. Kikon, N., Kumar, D. & Ahmed, S. A. Quantitative assessment of land surface temperature and vegetation indices on a Kilometer grid scale. *Environ. Sci. Pollut. Res.* **30** (49), 107236–107258. https://doi.org/10.1007/s11356-023-27418-y (2023).
33. Schwaab, J. et al. The role of urban trees in reducing land surface temperatures in European cities. *Nat. Commun.* **12** (1), 6763. https://doi.org/10.1038/s41467-021-26768-w (2021).
34. Ramachandra, T. V., Mondal, T., Settur, B. & Aithal, B. H. Environmental consequences in the neighbourhood of rapid unplanned urbanisation in Bangalore city. *Adv. Environ. Eng. Res.* **4** (4), 1–17. https://doi.org/10.21926/aeer.2304052 (2023).
35. Islam, S. et al. Urban heat Island effect in india: a review of current status, impact and mitigation strategies. *Discov. Cities*. **1**, 34. https://doi.org/10.1007/s44327-024-00033-3 (2024).
36. Bottyán, Z. & Unger, J. A multiple linear statistical model for estimating the mean maximum urban heat Island. *Theoret. Appl. Climatol.* **75**, 233–243. https://doi.org/10.1007/s00704-003-0735-7 (2003).
37. Lin, J., Wei, K. & Guan, Z. Exploring the connection between morphological characteristic of built-up areas and surface heat Islands based on MSPA. *Urban Clim.* **53**, 101764. https://doi.org/10.1016/j.uclim.2023.101764 (2023).
38. Landsat Data. (accessed 1 June 2025); https://landsat.gsfc.nasa.gov/data/handbooks-guides/
39. Sentinel data. (accessed 1 June 2025); https://sentinel.esa.int/documents/247904/685211/Sentinel-2_User_Handbook
40. The Karnataka Town and Country Planning Act. (accessed 5 June 2025); https://dpal.karnataka.gov.in/storage/pdf-files/11%20of%201963%20(E).pdf
41. The Comprehensive Development Plan (CDP). (accessed 5 June 2025); https://eng.bdabangalore.org/uploads/files/EODB/Additional%20document/Zonal%20Regulation%202007.pdf
42. The Revised Master Plan (RMP). Bangalore Development Authority. (accessed 5 June 2025); https://eng.bdabangalore.org/uploads/files/EODB/Additional%20document/Zonal%20Regulation%202007.pdf

43. Ramachandra, T. V. et al. Bangalore lakes information system (BLIS) for sustainable management of lakes. *J. Indian Inst. Sci.* **104**, 415–434. https://doi.org/10.1007/s41745-024-00444-6 (2024).
44. Ramachandra, T. V., Asulabha, K. S., Sincy, V. & Jaishanker, R. Wetlands for human well-being (Editorial), *J. Environ. Biol.* **45** (2), i-iv https://doi.org/10.22438/jeb/45/2/Editorial (2024).
45. Ramachandra, T. V. et al. *Natural Capital Accounting and Valuation of Ecosystem Services, Karnataka State, India* 674 https://doi.org/10.1007/978-981-97-2405-5_1 (Springer Nature, 2024).
46. Ramachandra, T. V. Rejuvenation of Lakes: Insights from the success story of Jakkur Lake. *Sarovar* **9**, 11–14 (2024).
47. Ramachandra, T. V. Innovative ecological approaches to ensure clean and adequate water for all (Editorial). *J. Environ. Biol.* **43** (3), i–ii. https://doi.org/10.22438/jeb/43/3/Editorial (2022).
48. Lin, J., Wang, Y., Lin, Z. & Li, S. National-scale connectivity analysis and construction of forest networks based on graph theory: A case study of China. *Ecol. Eng.* **216**, 107639 https://doi.org/10.1016/j.ecoleng.2025.107639 (2025).
49. The 74th Constitutional Amendment Act of 1992. Government of India. (accessed 5 June 2025); https://secforuts.mha.gov.in/74th-amendment-and-municipalities-in-india/
50. The Master Plan. Bangalore Development Authority. https://bdabangalore.org/uploads/files/TPM_Documents/RMP_2031/PLU_12.pdf (2031).
51. Nguyen, L. H., Joshi, D. R., Clay, D. E. & Henebry, G. M. Characterizing land cover/land use from multiple years of Landsat and MODIS time series: A novel approach using land surface phenology modeling and random forest classifier. *Remote Sens. Environ.* **238**, 111017. https://doi.org/10.1016/j.rse.2018.12.016 (2020).
52. Ramachandra, T. V., Negi, P. & Setturu, B. Insights from big spatial data through machine learning techniques for prudent management of natural resources. *J. Resour. Energy Dev.* **19** (1–2),1–18. https://doi.org/10.3233/RED-191201 (2022).
53. Breiman, L. Bagging predictors. *Mach. Learn.* **24**, 123–140. https://doi.org/10.1007/BF00058655 (1996).
54. Gislason, P. O., Benediktsson, J. A. & Sveinsson, J. R. Random forests for land cover classification. *Pattern Recognit. Lett.* **27** (4), 294–300. https://doi.org/10.1016/j.patrec.2005.08.011 (2006).
55. Rodriguez-Galiano, V. F., Ghimire, B., Rogan, J., Chica-Olmo, M. & Rigol-Sanchez, J. P. An assessment of the effectiveness of a random forest classifier for land-cover classification. *ISPRS J. Photogramm. Remote Sens.* **67**, 93–104. https://doi.org/10.1016/j.isprsjprs.2011.11.002 (2012).
56. Breiman, L. Random forests. *Mach. Learn.* **45**, 5–32. https://doi.org/10.1023/A:1010933404324 (2001).
57. Weng, Q., Lu, D. & Schubring, J. Estimation of land surface temperature–vegetation abundance relationship for urban heat Island studies. *Remote Sens. Environ.* **89** (4), 467–483. https://doi.org/10.1016/j.rse.2003.11.005 (2004).
58. Sharma, R., Pradhan, L., Kumari, M. & Bhattacharya, P. Assessing urban heat Islands and thermal comfort in Noida City using geospatial technology. *Urban Clim.* **35**, 100751. https://doi.org/10.1016/j.uclim.2020.100751 (2021).

Acknowledgements

We are grateful to the EIACP (ENVIS) Division, the Ministry of Environment, Forests and Climate Change, the Government of India for the partial financial (field data collection) and the Indian Institute of Science for infrastructure support.

Author contributions

Conceptualization, development of methods, soft computing, field investigation, validation, writing, formatting, and reviewing were carried out by all authors. All authors have read and agreed to the published version of the manuscript.

Funding

Field research is funded (partially) by the EIACP (ENVIS) division, the Ministry of Environment, Forests and Climate Change, Government of India, and infrastructure support is provided by the Indian Institute of Science.

Declarations

Competing interests

The authors declare no competing interests.

Additional information

Supplementary Information The online version contains supplementary material available at https://doi.org/10.1038/s41598-025-09141-5.

Correspondence and requests for materials should be addressed to T.V.R.